

# A multiregressed COA-SAM model for predicting seasonal streamflow variability: A case study over Murray river basin

Tufail M.Y.<sup>1</sup>, Gul S.<sup>1</sup>, Zia S.S.<sup>2</sup>, Jabeen L.<sup>2</sup> and Rasheed S.<sup>2</sup>

<sup>1</sup>Department of Mathematics, NED University of Engineering & technology, Karachi, Pakistan

<sup>2</sup>Department of Mathematics, University of Karachi, Karachi, Pakistan

Received: 25/08/2023, Accepted: 05/11/2023, Available online: 01/02/2024

\*to whom all correspondence should be addressed: e-mail: tufail@neduet.edu.pk

<https://doi.org/10.30955/gnj.005329>

## Graphical abstract



## Abstract

Streamflow of the Murray River (MR) was investigated from 1978 to 2017, using statistical analysis based on Indian Ocean modes of variability. During the cool season, June to August (JJA), observations and reanalysis products have been used to analyse the relation of streamflow of MR with Indian Ocean High (IOH) and Southern Annular Mode (SAM) over South Australia (SA). Recently, the river has suffered from severe drought, whereas drought drivers differ significantly in terms of interannual and decadal timescales. As a defining feature of atmospheric general circulation, the IOH is quantitatively simulated in all global climate models. Variations in the streamflow of MR have been linked to the variability of intensity and positions of Indian Ocean high pressure (IOHP) meridionally and the impact of SAM across the Indian Ocean. It is found that the correlation of streamflow with IOHP is ( $r = -0.41$ ), SAM ( $r = -0.52$ ) and shows the strongest correlation with Indian Ocean High Longitude (IOHLN), which is  $-0.56$ . Moreover, SAM explains only 27% of streamflow variability, while IOHP and IOHLN indices calculated by the Center of Action (COA) approach explain 39% of the variation. This paper examines the decline of the inflow rate of MR in SA by applying the COA approach, Mann-Kendall (MK) test and Pearson correlation. We further investigate the impact of significant predictors

over the flow of MR. Inflow rate of the hydrology of MR is influenced by the period of time, which shows a decreasing trend with  $-1.976$  by applying autocorrelation. Overall, monthly and annual streamflows have also investigated a significant decreasing trend. Cross-correlation is also used to verify the relationship between streamflow and significant predictors of MR.

**Keywords:** Murray river, center of action approach, south annular mode, streamflow, Indian Ocean high

## 1. Introduction

The Australian climate is distinguished by a dry to semi-humid state for a huge part of the continent. The research from the last decades made it evident that the extreme dry season in Australia is not irregular but intensely influenced by circular climatic patterns. The pattern considered most is El Niño Southern Oscillation (ENSO), (McGowan, Marx, Denholm, Soderholm & Kamber, 2009). Indeed so, the strength of the dry season mostly observed over Southeast Australia (SEA) and Southwest Western Australia (SWWA) appears unusual for its stability (Murphy and Timbal, 2008; Sohn, 2007). The significantly influenced Murray River (MR) streamflow is a major water resource framework for Australia, with approximately three-quarters of the SA's water system and the rest of Australia's population depending on 40% of water, as mentioned by Australian Bureau of Agricultural and Resource Economics (2006). According to CSIRO (2008), the effluence of streamflow from the MR framework decreased to 48% below the normal flow in the last decades. Consequently, rural and urban regions of Australia have experienced social and environmental effects, such as sustainable use of freshwater, a decline in crop cultivation, substantial harm to the ecosphere, and increased wildfire incidents (Leblanc, Tregoning, Ramillien, Tweed, & Fakes, 2009). This current dry spell in SEA is considered the most severe and dreadful disaster for Australia, and the event is named "Big Dry", as mentioned in the literature (Sohn, 2007; LeBlanc et al., 2009). Moreover, the streamflow of the Murray-Darling Basin has drastically declined in the SEA, which directly impacts the low flow of rivers towards inland regions, including

most areas of the SA. Precipitation is a significant source of streamflow, which is exceeded by evaporation and windswept salt, stowed over the Indian Ocean surface, shifting laden of about 120 kg/m<sup>2</sup> as mentioned by (Stokes, Stone, & Loh, 1980). The three major headwaters in SA are Swan Avon River, Murray River, and Blackwood River.

The Murray River (MR) is Australia's longest river, located near the Southern tip of the Australian continent, that stretches 2,700 kilometres from the mountains of North-eastern Victoria to near Adelaide in SA, drains over one million hectares (one-seventh of Australia), as mentioned by Mackay and Eastburn (1990), which can be seen in the catchment Figure 1. Besides semiarid lowlands, the said area consists of Australia's two longest rivers, the Murray and Darling. The flow of many rivers in the Basin is regulated for anthropogenic purposes. There is also considerable agricultural production within the Basin, and the clearing of aboriginal herbage has significantly impacted over water quality of the rivers, particularly in terms of salinization (Mackay & Eastburn, 1990; Young, 2001). A diverse group of stakeholders relies heavily on it for their livelihoods as a complex economic and natural resource. The Basin Authority of MR estimates up to 47,161ml/day can be extracted for water usage, mainly for irrigation purposes that produced 1.8 billion Australian dollars by irrigation of crops along the main channel of MR from 2005-06 as determined by the Australian Bureau of Statistics (2009). According to the International Ramsar Convention, numerous other wetlands provide breeding and feeding grounds for birds, including habitation for marine life, as mentioned by CSIRO (2008). The MR has provided water to many of its habitants which has been carefully managed in its water regimes. The Eaton and Murray River Commission commissioned large storages and weirs to aid navigation and rerouting water for fertilization in the upper to lower reaches in 1945. For considerable fluctuation of effluence, water management plans were also devised. Water allocation is used to control wasteful water consumption. According to Chiew, Zhou, and McMahon (2003), the use of seasonal water supply accessibility forecasts can benefit many aspects of water management.

Moreover, it is crucial to understand the factors responsible for the drought cycle in Australia as the causes of "Big Dry" is still the most important debate. The Big Dry over Australia has also been followed by a persistent reduction in precipitation during autumn over SEA as mentioned by Murphy and Timbal (2008). According to Cai, Sullivan, and Cowan (2008), the southern climatic factors have influenced over rainfall of Australia by the fluctuations of El Niño (La Niña) episodes. Furthermore, a decrease in northwestern clouds formation associate with semiarid anomalous temperature patterns, presumably by serious admonition of the Indian Ocean. According to Cai, Cowan, and Sullivan (2009), the positive Indian Ocean dipoles have been influenced since the half of the 20<sup>th</sup> century that causes variations in the austral winter and spring of SA. There is a significant association between anomalous

SAM's behavior and drought conditions in SWWA and SEA (Gallant, Kiem, Verdon-Kidd, Stone, & Karoly, 2011; Murphy & Timbal, 2008; Verdon-Kidd & Kiem, 2009), and this will become more common under global warming as mentioned by Cai, Shi, Cowan, Bi, and Ribbe (2005).

Furthermore, Nicholls (2010) has mentioned that precipitation trends over Australia depend on the increase in pressure, feasibly influenced by increasing SAM positively, and this could account for over 70% of the decrease in rainfall. SAM has the greatest impact on increasing trends in SA winter rainfall (Hendon, Thompson, & Wheeler, 2007; Meneghini, Simmonds, & Smith, 2007). A notable understanding of perforation surrounding about Australian climate that can be associated with SAM, as well as how SAM could influence Australia's environment in the future, and it is necessary to provide correlated climate models globally and regionally for understanding the role of SAM in Australian climate factors as discussed by Kiem and Verdon-Kidd (2011). Rice and Emanuel (2017) found a string relation of streamflow with ENSO and related climatic variables, although the correlation trend decreases with time.

Furthermore, it is also determined that the Center of Action (COA) is the most practiced approach to investigate various regional phenomena. Hameed, Iqbal, Rehman, and Collins (2011) have shown the influence of Indian Ocean High Pressure (IOHP) and its longitude position (IOHLN) over winter precipitation in WA from 1951 to 2008 by applying the COA approach. This method calculates three objective indices (intensity, latitude, and longitude) of high or low-pressure systems using quantitative analysis. A significant influence over the streamflow of the Donnelly River in SA is caused by fluctuations in the IOHLN (Rehman & Iqbal, 2011). Furthermore, Australian precipitation decreases due to this southward shift in all seasons (Rehman, Khan, & Simmonds, 2019). As a result of COA, we can estimate fluctuations in pressure over the Indian Ocean, as well movement of pressure centres. A variety of studies have used this method to investigate ocean-atmospheric interactions (Doherty, Riemer, & Hameed, 2008; Hameed & Piontkovski, 2004; Hameed *et al.*, 2011; Rehman, 2014; Riemer, Doherty & Hameed, 2006).

The purpose of this article is to examine the factors associated with drought in Australia's largest catchment area, the Murray Darling Basin, which is associated by the pressure circular patterns of Indian Ocean. For this purpose, streamflow data of MR is obtained from Hydrological Resource Stations (HSR) and climate indices data from the National Center of Environmental Prediction (NCEP). Moreover, the COA approach is applied to calculate the intensity and position of high-pressure centers of the Indian Ocean. Furthermore, statistical analysis is applied to analyze the significant relationship between the streamflow of MR. Each of the climatic predictors related to pressure circular patterns of the Indian Ocean shows a significant impact which is further investigated and verified by applying the Variance Inflation Factor (VIF) to analyze separately. Mann Kendall

test is also used to analyze the trend of streamflow in the winter season. Significant findings are further substantiated by applying Cross-lagged correlation. Thus, we have achieved notable results which show a strong relationship between the streamflow of MR with strongly correlated predictors (IOHP, IOHLN and SAM).

## 2. Data

### 2.1. Stream flow datasets

The Australian Bureau of Meteorology developed Hydrological Resource Stations (HSR), which provide a compilation of daily discharge records that were relatively free of anthropogenic influences like watercourse regulation, diversion, groundwater pumpage, or land occupied variations. Monthly mean datasets are downloaded from the following link:

<http://www.bom.gov.au/water/hrs/#panel=datadownload&id=614006>

As mentioned by Rehman (2014). HRS consists of stations from eight major regions that are New South Wales (NSW), Victoria (VIC), Queensland (QLD), South Australia (SA), Western Australia (WA), Tasmania (TAS), Northern Territory (NT) and Australian Capital Territory (ACT) including many basins and catchment area of 50km<sup>2</sup> to 2000km<sup>2</sup>. In this article, we have obtained stream flow data of Murray Darling Basin (MDB) consisting of NSW, VIC, QLD, and SA from 1978 to 2017, as displayed in Figure 1. We have normalized the streamflow data according to the catchment area to make it easier to analyze the inflow of MR.

### 2.2. Indian ocean high

A series of internal quality tests are conducted on streamflow station data before being used to develop the topography-resolving dataset. As streamflow of MDB is affected by the pressure system of the Indian Ocean High. Therefore, this study has used monthly mean gridded sea level pressure datasets of spatial resolution of 2.5° × 2.5°, obtained from the National Center of Environmental Prediction (NCEP) as discussed by Kalnay *et al.* (1996), for calculating COA objective indices of Indian Ocean High Pressure (IOHP), Indian Ocean High Longitude (IOHLN) and Indian Ocean High Latitude (IOHLT) as explained by Hameed and Piontkovski (2004). Where IOHP represents intensity, and IOHLN and IOHLT represent the position of pressure. NCEP reanalysis has provided composite maps which helped us to analyze the magnitude and direction of the pressure system at a particular region.

### 2.3. Global circulation indices

Streamflow of MDB also relates with other climate indices like the Multivariate ENSO Index (MEI), Southern Annular Mode (SAM), Southern Oscillation Index (SOI) and Dipole Mode Index (DMI). The DMI, ENSO and SOI indices are obtained from NCEP ([www.cpc.ncep.noaa.gov](http://www.cpc.ncep.noaa.gov)). SAM indices are available from several sources. In contrast, we used the particular index that has more observations compared with other datasets, as mentioned by Marshall (2003), obtained from David Thompson's website. All datasets in this paper are calculated and analyzed,

particularly for the winter season from June to August (JJA).

## 3. Methods

### 3.1. Rossby model

The Center of Action (COA) approach analyses the quantitative impact of fluctuations of pressure centers in the ocean along the longitude and latitude positions. Hameed *et al.* (2011) applied this method to examine the intensity and position of the pressure center of IOH. According to Santer (1988) and Hameed, Shi, Boyle, and Santer (1995), the pressure index ( $I_p$ ) of a high-pressure system is defined as a region occupied by pressure departure from a threshold value over a domain ( $i, j$ ) as mentioned in Equation (1):

$$I_{p,\Delta t} = \frac{\sum_{i=1}^I \sum_{j=1}^J (P_{ij,\Delta t} - P_t) \cos \Phi_{ij} \delta_{ij,\Delta t}}{\sum_{i=1}^I \sum_{j=1}^J \cos \Phi_{ij} \delta_{ij,\Delta t}} \quad (1)$$

Here  $P_{ij, \Delta t}$  represents the average sea level pressure at each grid ( $i, j$ ) over time  $\Delta t$ . Whereas data values are obtained from NCEP reanalysis, and  $P_t$  represents a constant threshold value of 1016hPa.  $\Phi_{ij}$  shows the latitude of the pressure system at point ( $i, j$ ).  $\Phi_{ij}$  and  $\lambda_{ij}$  represent the latitude and longitude positions of pressure at grid points ( $i, j$ ) respectively. Such that  $\delta = 1$  if and only if  $(P_{ij, \Delta t} - P_t) > 0$ , in other way when  $\delta = 0$ , then  $(P_{ij, \Delta t} - P_t) < 0$ , which causes variations in the pressure system of the Indian Ocean. It is important to understand that when identifying High pressure centres, this process eliminates all points associated with adjacent Low pressure centres, and vice versa when identifying Low pressure centres. The magnitude is consequently representing the quantification of analogous values of the pressure system at point ( $i, j$ ). The boundary of Indian Ocean High is enclosed as 10°S to 45°S and 40°E to 120°E. Value  $P_t$  is considered by analyzing previous historical data of pressure from NCEP reanalysis.

Similarly, Equation (2) shows the latitudinal position of pressure as the intensity of pressure which is defined above in Equation (1).

$$I_{\Phi,\Delta t} = \frac{\sum_{i=1}^I \sum_{j=1}^J (P_{ij,\Delta t} - P_t) \Phi_{ij} \cos \Phi_{ij} \delta_{ij,\Delta t}}{\sum_{i=1}^I \sum_{j=1}^J (P_{ij,\Delta t} - P_t) \cos \Phi_{ij} \delta_{ij,\Delta t}} \quad (2)$$

and  $I_{\lambda, \Delta t}$  represents the longitudinal index of pressure in Equation (3).

$$I_{\lambda,\Delta t} = \frac{\sum_{i=1}^I \sum_{j=1}^J (P_{ij,\Delta t} - P_t) \lambda_{ij} \cos \Phi_{ij} \delta_{ij,\Delta t}}{\sum_{i=1}^I \sum_{j=1}^J (P_{ij,\Delta t} - P_t) \cos \Phi_{ij} \delta_{ij,\Delta t}} \quad (3)$$

### 3.2. Mann kendall test

The Mann-Kendall statistical test is used to analyze the increasing or decreasing trend of data values over time. This test also helps to examine whether data is significant or insignificant and it is mainly known as Kendall's tau statistic test. Kendall tau test is the most frequently applied test for climatological time series as mentioned by Zhang, Harvey, Hogg, and Yuzyk (2001). In this technique, the null Hypothesis ( $H_0$ ) represents the trend of data values ( $X_1, \dots, X_n$ ) which is independent of  $n$  and arranged

for random values of the dataset as discussed by Yu, Zou, and Whittemore (1993). Two tail test is analyzed by considering the alternative Hypothesis ( $H_1$ ), which described that  $x_j$  and  $x_k$  are not arranged likely for  $j, k \leq n, \forall k \neq j$ . This statistical test (S) is determined by the given equations:

$$S = \sum_{k=1}^{n-1} \sum_{j=k+1}^n \text{sgn}(x_j - x_k) \quad (4)$$

$$\text{sgn}(x_j - x_k) = \begin{cases} +1 & \text{if } (x_j - x_k) > 0 \\ 0 & \text{if } (x_j - x_k) = 0 \\ -1 & \text{if } (x_j - x_k) < 0 \end{cases} \quad (5)$$

In the above equations, the mean is zero and the variance of 'S' can be calculated by,

$$\text{Var}(S) = [n(n-1)(2n+5) - \sum_t t(t-1)(2t+5)]/18 \quad (6)$$

Which is considered normal as described by Hirsch and Slack (1984). Here 't' represents any tie and  $\sum t$  represents the summation of all ties. For this method number ( $n$ ) of data values must be larger than 10,  $n > 10$ . Furthermore, the standard normal variation (Z) is calculated by the Equation given below:

$$Z = \begin{cases} \frac{S-1}{\sqrt{\text{var}(S)}} & \text{if } S > 0 \\ 0 & \text{if } S = 0 \\ \frac{S+1}{\sqrt{\text{var}(S)}} & \text{if } S < 0 \end{cases} \quad (7)$$

Therefore, the two-tailed test is used for analyzing the trend,  $H_0$  is accepted if  $|Z| \leq Z_{\alpha/2}$  at a 5% significant level. If  $S > 0$ , a positive trend is obtained and for  $S < 0$ , a negative or decreasing trend is shown.

### 3.3. Variance inflation factor (VIF)

The intensity of multicollinear findings is investigated by calculating Variance Inflation Factor (VIF) by the following formula:

$$\text{VIF}_j = \frac{1}{\sqrt{1-R_j^2}} \quad (8)$$

Here  $R^2$  represents a multiple correlation coefficient that corresponds to the variance associated with the  $j$ th predictor compared to the remaining  $p-1$  predictors. If  $R_j^2=0$ , all  $j$ th predictors remain orthogonal (independent). Since  $R^2$  approaches to zero represents weak correlations. Therefore, VIF is closer to 1 and shows weak multicollinearity. Furthermore,  $\text{VIF} > 5$  shows a high linear correlation between the predictors as explained by Vu, Muttaqi, and Agalgaonkar (2015).

## 4. Results and discussion

To assess the alteration of hydrologic regimes, which can be constructed by hydrologic metrics. For this purpose, the histogram of streamflow from 1978 to 2017 is constructed and displayed in Figure 2, where a positively skewed graph is formed. The average flow of Murray River (MR) from the last few decades is observed on a monthly basis; each bar of bar chart displays the mean streamflow of each month from 1978 to 2017 in Figure 3. We observe

the highest bars in the months of August and July which represents the heavy flow of MR. Hence, to further analyze flow in different seasons, a seasonal bar graph is generated in Figure 4, representing heavy flow in the winter (Jun to August) season in Murray River through the height of bars. Recently, Australia is suffered from drought, known as the "Big drought", as mentioned in the previous section. In the last few decades, winter rainfall has immensely declined in the initial stages of the winter. However, winter precipitation in the late winter season remained relatively stable, as discussed by Indian Ocean Climate Initiative-Western Australia (2004) and Li, Cai, and Campbell (2005). We have further observed the trend of streamflow of MR in the winter season by applying the Mann-Kendall test as the equations of this test are mentioned above. We have applied this test to examine variations and Sen's slope of streamflow. Z and Sen's slope values are distributed according to stations at above mentioned time scales that are found negative which exhibits decreasing trend with  $p < 0.05$ , as displayed in Figure 5, with a variation of -1.967.

As streamflow is affected by various climatic variables and these variables are computed by Pearson correlation. So, we used statistical approaches to analyze the relationship between streamflow, ENSO climate variables, and COA indices. Figures 6a and 6b represent the correlation of stream flow of JJA in Raw and Detrended forms with Time parameter, as well as with the COA's indices of IOH by position and strength (IOHP, IOHLN, and IOHLT), and related ENSO climate variables (i.e., MEI, SAM, DMI, SOI, Nino 3, Nino 1+2, Nino 3.4, and Nino 4) for the above mentioned time period. We found a strong negative correlation of streamflow with IOHP, IOHLN, and SAM. The correlations between streamflow of MR during the winter (July to August) season shows Pearson correlation of IOHP ( $r = -0.41$ ), IOHLN ( $r = -0.56$ ), and the correlation with SAM, observed at  $-0.52$  at  $p < 0.05$ . As IOH has a negative impact on the streamflow of MR which shows streamflow increases as the IOHP shifts westward and in reverse situation pressure centre of IOH shifts may result in a reduction of streamflow. Reduced precipitation was persuaded by shifting towards the East which can also be seen by the negative correlation of SAM that indicates movement towards the Southeast of Australia. Moreover, we got the same results by taking the z-score of the above-mentioned climatic variables, as shown in Figure 6b.

The Indian Ocean High pressure represents the Hadley Circulation and variations in the Hadley Circulation that can be seen as a result of the multi-decadal strengthening of the IOH. In both hemispheres, subtropical dry regions move towards dipoles of IOH due to the shifting of the Hadley circulation since 1979 (Birner, Davis, & Seidel, 2014; Grise, Davis, Staten, & Adam, 2018; Grise *et al.*, 2019; Lucas, Timbal, & Nguyen, 2014).

The multiple linear regression model is based on fitting a linear equation to the linear relationship between the explanatory (independent) variables and the response (dependent) variables as mentioned by Andrews (1974). The dependent variables represent the streamflow of MR

in the winter season and the independent variables IOHP, IOHLN, and SAM are considered significant, with 44% variability with streamflow. We also develop the following relation for winter streamflow by using multiple regression against IOHP, IOHLN, and SAM in Equation 9.

$$\text{Streamflow (ML / month)} = 21775599 - (18345) * \text{IOHP} - (31313) * \text{IOHLN} - (26023) * \text{SAM} \quad (9)$$

Based on the multicollinear regression model in Equation 9 shows the streamflow of Murray River depends on three significant variables, as significant predictors of Tasmania rainfall is analyzed through a multilinear model by Rehman *et al.* (2019). This model comprises three significant predictors that are not fully expressed in basin information. Whereas a linear model with more than two variables can be inefficient and unstable to analyze. Therefore, we suppose  $R_j$  as the multiple correlation coefficient that corresponds to the variance associated with the  $j$ th predictor and is compared to the remaining  $p-1$  predictors. If  $R_j^2 = 0$ , all  $j$ th predictors are orthogonal (independent). A regression model with predictors can calculate the values of a multilinear model and the method for examining multicollinearity is the variance inflation factor (VIF). The redundant features with low variance are removed to avoid a complex model while providing enough information to prevent accuracy loss. Each predictor's variance that is found significant in Figures 6a and 6b is quantified by applying the VIF technique; values are mentioned in Table 1 by reconstruction of linear-correlated variables on an individual basis. Principal components (PC) of IOHLN with smaller VIF are excluded by principal component analysis (PCA), resulting in meridional movement of the pressure centre. VIF values are within (1.0–1.5) which is an acceptable range with significant test results of  $p \geq 0.10$ , suggesting the balanced model at  $R^2 \leq 0.05$ .

A lag with the highest correlation coefficient represents the best fit between the two series. It is the lag times sampling interval that determines how long the effect of a variable takes to propagate from one variable to another. According to the autocorrelation function data points in a time series are associated with the average of the preceding data points as mentioned by (Jenkins, Ferrier, Harriman, & Ogunkoya, 1994). It measures the signal's self-similarity over different delay times. Figure 7 represents fluctuations in streamflow from 1978 to 2017. Thus, the autocorrelated function (ACF) is a function of the delay or lag  $\tau$ , which determines the time shift taken into the past to estimate the similarity of the function over time.

Moreover, there are many variables that describe how well data fits together, including correlation coefficients. Whereas cross-correlation is one of the most useful method to analyze cross-correlation factor (CCF) represents constancy at maximum  $R^2$  between streamflow and the significant factors. In contrast, lag measures the timing delay of the circular pressure patterns response relative to the stream discharge. The highest  $R^2$  value indicates synchronized waveforms and a similar structure

of the graph as displayed in Figure 8. Despite this cross-correlation, it provides a simple, direct, and consistent approach to forecast streamflow with ENSO in advance techniques for comparison by other statistical methods. Catchments that have IOH-streamflow teleconnections (high amplitudes in the first harmonic fit) also have high lag correlations between streamflow and ENSO, which can be observed in Figure 8. The cross-correlation of streamflow at lag 12 is negatively correlated with IOHP, IOHLN and SAM. Cross-correlation of Figures 8a and 8b shows fidelity response. Whereas cross-correlation with SAM shows a slightly moderate response. These strongly influenced indices provide significant and stable correlations with streamflow at Lag 12, with those associated variables using the ENSO phenomenon showing the highest negative correlation.

## 5. Forecasting the Mr Flow

In this section, we build a multiple regression model for forecasting streamflow in rivers using IOHP and IOHLN. We can see the values of the IOHP and IOHLN series with respect to time (years) in Figures 9a and 9b respectively. The above analysis provided a significant relationship between IOHP and IOHLN with streamflow data. Now we predict the streamflow values using IOHP and IOHLN as continuous predictors. Figure (10) captures the values of observed versus predicted values. It is important to note that multiple regression models have limitations and assumptions, and their accuracy depends on the quality and quantity of the data, as well as the appropriateness of the model assumptions for the specific case. Our regression model best captures the values in 1969, 1981 and 1996. This analysis provides the basis that if we are able to predict the next year pressure values, the flow of the next year can predict up to an accurate level.

## 6. Conclusions

This study demonstrates the analysis of responsible factors that are associated with the flow of the Murray River (MR), Australia, from 1978 to 2017. In this paper, we develop and assess statistical methods for analysing irregular inflows of the Murray River. Results indicate that ENSO tends to cause droughts in the streamflow of Murray-Darling Basin, Australia. Heavily inflow of streamflow is found in the winter (June to August) season. Whereas Australia has suffered from a "Big Drought" in the last few decades, which has been examined by applying various statistical techniques from different perspectives. The center of Action (COA) approach is used to examine the pressure centre of Indian Ocean High (IOH) along with its intensity and position. Climatic variables of ENSO are examined by correlation technique which shows a pressure of IOH meridionally, and Southern Annular Mode (SAM) are inversely proportional to the flow of MR at 5% of significant level with 44% variability. The trend of winter streamflow of MR is observed by applying the Mann-Kendall test. Autocorrelation and cross lagged correlation are also applied to find the constancy and time delay of significant predictors over streamflow. The cross-correlation factor (CCF) indicates that the

estimation of cross-covariances and autocorrelations of the logarithms of observations can lead to a strong analysis of the authentic cross-correlations and autocorrelations of flows in sample estimation. CCF also suggests that significant ENSO indicators can be used to predict streamflows, which results in a significant leadtime.

In some regions, it may also be possible to obtain higher lag correlations. There may be a relationship between streamflow and ENSO indicators more appropriate to the region (such as sea surface temperature or atmospheric pressure) rather than SOI or MEI can be analyzed in future. Possibly the maximum crucial lesson to learn from research is that analyses over multiple streamflows along with parameters cannot be properly investigated, as mentioned by Stedinger (1980). This forecast estimation seems robust for a strong relationship to the lengthy time period for all, but mainly for the winter season.

**Acknowledgement**

The authors would like to thank Australian Bureau of Meteorology, department of water for providing monthly streamflow data.

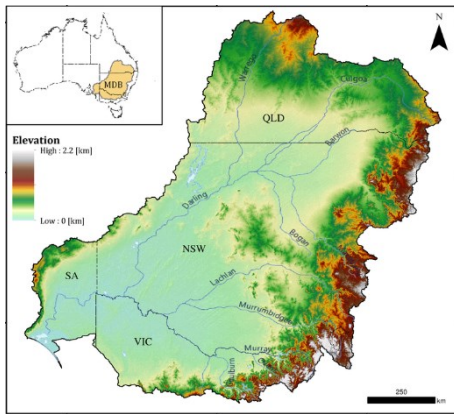


**Figure 1.** Location of Murray River station and main tributaries used in this study

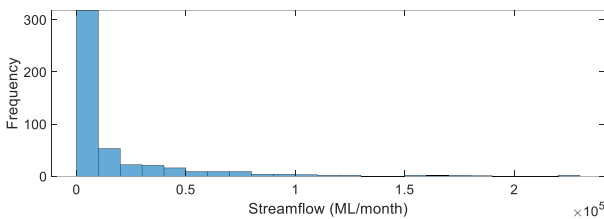


**Figure 2.** Histogram shows monthly mean flow of Murray River from 1978 to 2017

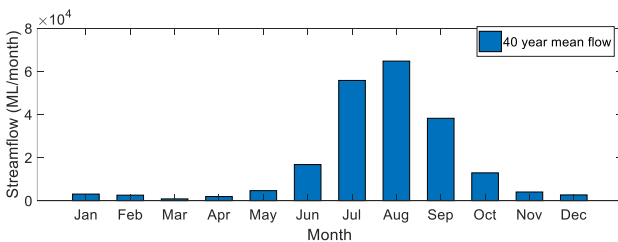


**Figure 3.** Comparison of streamflow of Murray River from 1978 to 2017 in each month through bars. Heavy flow is observed in July and August

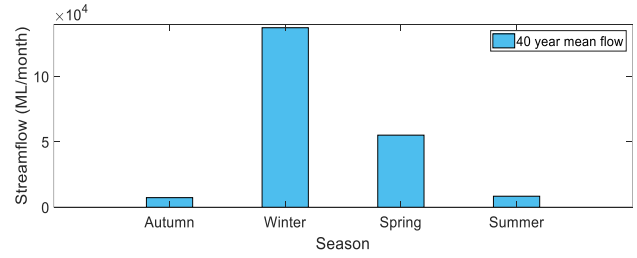


**Figure 4.** Seasonal Bar graph shows streamflow of Murray River for 1984 – 2017 where comparatively winter (JJA) season represents excess flow

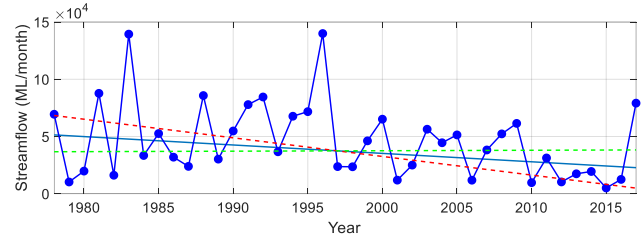


**Figure 5.** Illustrates Mann-Kendall trend test results from 1978-2017 for Winter (Jun-August) show a negative trend over -1.96 is significant at the 0.05 level of significance

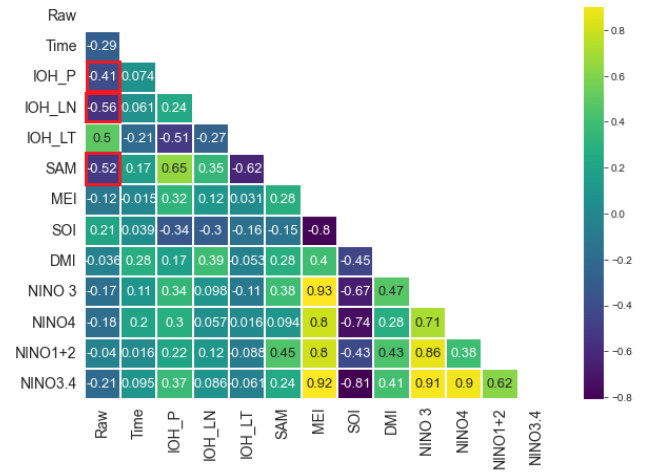


**Figure 6a.** Heatmap of Pearson correlation coefficients of Streamflow of Murray river versus response variable of all Southern Climatic variables

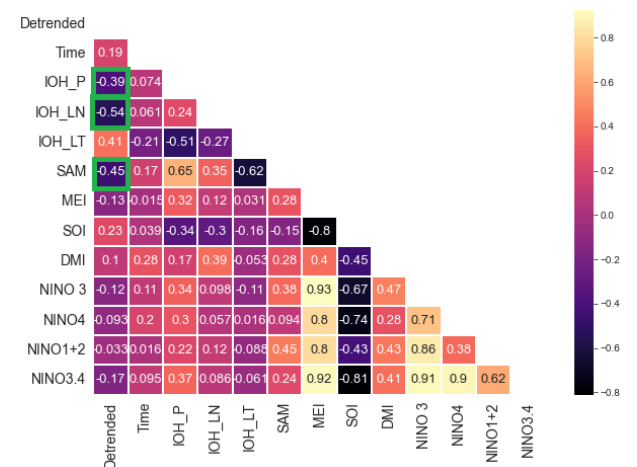


**Figure 6b.** Heatmap of Pearson correlation coefficients of dependent variable versus response variable of all southern climatic variables. The dependent variable is the detrended form of the monthly mean streamflow of the Murray River in JJA

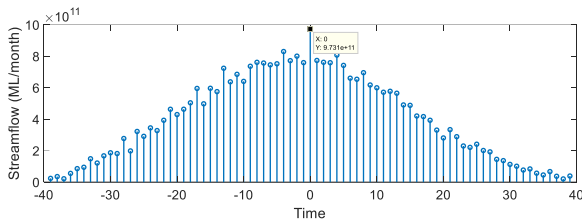


**Figure 7.** Cross-correlation of streamflow data of the Murray River from 1978 to 2017 in winter (JJA) season where highest mean position has been indicated

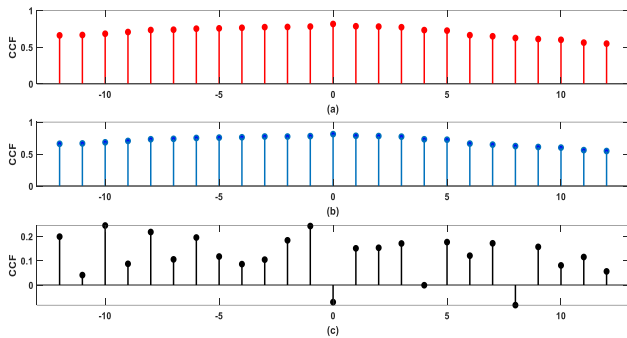


**Figure 8.** The correlation coefficient of cross correlation factor (CCF) represents (a) Lagged correlation between Streamflow and IOHP (b) Streamflow and IOHLN (c)

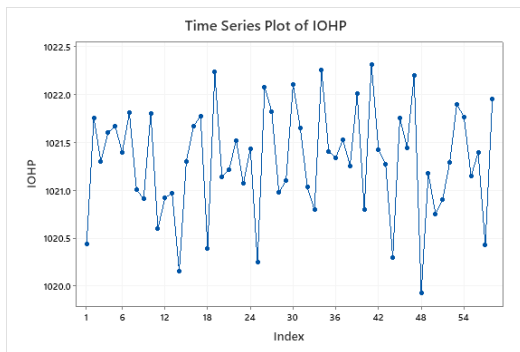


**Figure 9a.** Time series plot for IOHP reflects the forecasting for streamflow

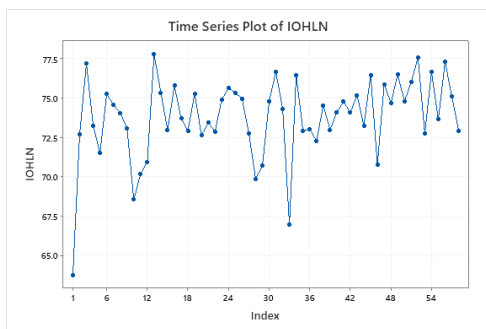


**Figure 9b.** Time series plot for IOHLN with respect to time (in years)

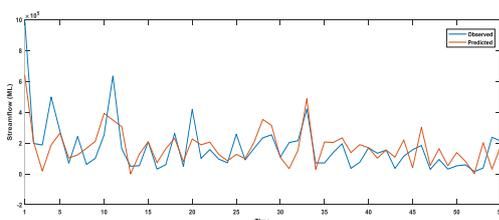


**Figure 10.** Comparison between predicted values (red) and observed values (blue)

**Table 1.** representing regression analysis for significant predictors of stream flow of Murray River from 1978 to 2017

Term	Coefficient	SE Coefficient	T Value	P-Value	VIF
Constant	21775599	25832791	0.84	0.405	-
IOHP	-18345	25314	-0.72	0.473	1.72
IOHLN	-31313	9834	-3.18	0.003	1.14
SAM	-26023	14861	-1.75	0.088	1.85

**References**

Australian Bureau of Agricultural and Resource Economics. (2006). Australian crop and livestock report 2006-07, drought update. Project No. 1076. *Australian Bureau of Agricultural and Resource Economics*: Canberra, 15.

Andrews D.F. (1974). A Robust Method for Multiple Linear Regression. *Technometrics*, **16**(4),523–531.Doi: <http://dx.doi.org/10.1080/00401706.1974.10489233>

Australian Bureau of Statistics. (2009). *Murrumbidgee sustainable yields region socioeconomic profile, report for the Murray–Darling Basin* Authority by the Australian Bureau of Statistics, Australian Bureau of Agricultural and Resource Economics & Bureau of Rural Sciences, Adelaide.

Birner T., Davis S. and Seidel D. (2014). The changing width of Earth's tropical belt. *Physics Today*, **67**, 38–44. Doi: <https://doi.org/10.1063/PT.3.2620>

Cai W., Cowan T. and Sullivan A. (2009). Recent unprecedented skewness towards positive Indian Ocean Dipole occurrences and its impact on Australian rainfall. *Geophysical Research Letters*, **36**(11). Doi: <https://doi.org/10.1029/2009GL037604>

Cai W. and Cowan T. (2006). SAM and regional rainfall in IPCC AR4 models: Can anthropogenic forcing account for southwest Western Australian winter rainfall reduction? *Geophysical Research Letters*, **33**(24). Doi: <https://doi.org/10.1029/2006GL028037>

Cai W., Sullivan A. and Cowan T. (2008). Shoaling of the off-equatorial south Indian Ocean thermocline: Is it driven by anthropogenic forcing? *Geophysical Research Letters*, **35**(12). Doi: <https://doi.org/10.1029/2008GL034174>

Cai W., Shi G., Cowan T., Bi D. and Ribbe J. (2005). The response of the Southern Annular Mode, the East Australian Current, and the southern mid-latitude ocean circulation to global warming. *Geophysical Research Letters*, **32**(23). Doi: <https://doi.org/10.1029/2005GL024701>

Chiew F.H.S., Zhou S.L. and McMahon T.A. (2003). Use of seasonal streamflow forecasts in water resources management. *Journal of Hydrology*, **270**(1):135–44. Doi: [https://doi.org/10.1016/S0022-1694\(02\)00292-5](https://doi.org/10.1016/S0022-1694(02)00292-5)

CSIRO. (2008). Water availability in the Murray-Darling Basin. Summary of a report from CSIRO to the Australian Government. Retrieved from <https://publications.csiro.au/rpr/download?pid=legacy:683 & dsid=DS1>

Doherty O.M., Riemer N. and Hameed S. (2008). Saharan mineral dust transport into the Caribbean: Observed atmospheric controls and trends. *J. Geophys. Res.*, **113**. Doi: <https://doi.org/10.1029/2007JD009171>

Gallant A.J.E., Kiem A.S., Verdon-Kidd D.C., Stone R.C. and Karoly D.J. (2011). Understanding climate processes in the Murray-Darling Basin: utility and limitations for natural resources management. *Hydrometeorology & Earth System Sciences Discussion*, **8**(4). Doi: <https://doi.org/10.5194/hessd-8-7873-2011>

- Grise K.M., Davis S.M., Staten P.W. and Adam O. (2018). Regional and Seasonal Characteristics of the Recent Expansion of the Tropics. *Journal of Climate*, **31**(17), 6839–6856. Doi: <https://doi.org/10.1175/JCLI-D-18-0060.1>
- Grise K.M., Davis S.M., Simpson I.R., Waugh D.W., Fu Q., Allen R.J., Rosenlof K.H., Ummenhofer C.C., Karnauskas K.B., Maycock A.C. and Quan X.W. (2019) Recent Tropical Expansion: Natural Variability or Forced Response? *Journal of Climate*, **32**(5), 1551–1571. Doi: <https://doi.org/10.1175/JCLI-D-18-0444.1>
- Hameed S. and Piontkovski S. (2004). The dominant influence of the Icelandic Low on the position of the Gulf Stream northwall, *Geophysical Research Letters*, **31**(9). Doi: <https://doi.org/10.1029/2004GL019561>
- Hameed S., Shi W., Boyle J. and Santer B. (1995). Investigation of the Centers of Action in the North Atlantic and the North Pacific. Proceedings of the *First International AMIP Scientific Conference, Monterey, California*. Retrieved from <https://pcmdi.llnl.gov/mips/amip/abstracts/Hameed95.html>
- Hameed S., Iqbal M.J., Rehman S. and Collins D. (2011). Impact of the Indian Ocean High Pressure System on winter precipitation over Western Australia and Southwest Western Australia. *Australian Meteorological and Oceanographic Journal*, **61**, 159–170. Doi: <https://doi.org/10.22499/2.6103.002>
- Hendon H.H., Thompson D.W.J. and Wheeler M. C. (2007). Australian Rainfall and Surface Temperature Variations Associated with the Southern Hemisphere Annular Mode. *Journal of Climate*, **20**(11), 2452–2467. Doi: <https://doi.org/10.1175/JCLI4134.1>
- Hirsch R.M. and Slack J.R. (1984). A Nonparametric Trend Test for Seasonal Data With Serial Dependence. *Water Resources Research*, **20**(6), 727–732. Doi: <https://doi.org/10.1029/WR020i006p00727>
- Indian Ocean Climate Initiative-Western Australia. (2004). *18th panel meeting sets agenda to broaden dialogue on climate change*, Bulletin no. 4. Retrieved from [http://www.ioici.org.au/pdf/IOCI\\_Bulletin4.pdf](http://www.ioici.org.au/pdf/IOCI_Bulletin4.pdf)
- Jenkins A., Ferrier R.C., Harriman R. and Ogunkoya Y.O. (1994). A case study in catchment hydrochemistry: Conflicting interpretations from hydrological and chemical observations. *Hydrological Processes*, **8**(4), 335–349. Doi: <https://doi.org/10.1002/hyp.3360080406>
- Kalnay E., Kanamitsu M., Kistler R., Collins W., Deaven D., Gandin L., Iredell M. and Joseph D. (1996). The NCEP/NCAR 40-Year Reanalysis Project. *Bull. Amer. Meteor. Soc.*, **77**, 437–471. Doi: [https://doi.org/10.1175/1520-0477\(1996\)077<0437:TNYRP>2.0.CO;2](https://doi.org/10.1175/1520-0477(1996)077<0437:TNYRP>2.0.CO;2)
- Kiem A.S. and Verdon-Kidd D.C. (2011). Steps toward useful hydroclimatic scenarios for water resource management in the Murray-Darling Basin. *Water Resources Research*, **47**(12). Doi: <https://doi.org/10.1029/2010WR009803>
- Leblanc M.J., Tregoning P., Ramillien G., Tweed S.O. and Fakes A. (2009). Basin-scale, integrated observations of the early 21st century multiyear drought in southeast Australia. *Water Resources Research*, **45**(4). Doi: <https://doi.org/10.1029/2008WR007333>
- Li Y., Cai W. and Campbell E.P. (2005). Statistical Modeling of Extreme Rainfall in Southwest Western Australia. *Journal of Climate*, **18**(6), 852–863. Doi: <https://doi.org/10.1175/JCLI-3296.1>
- Lucas C., Timbal B. and Nguyen H. (2014). The expanding tropics: a critical assessment of the observational and modeling studies. *WIREs Climate Change*, **5**(1):89–112. Doi: <https://doi.org/10.1002/wcc.251>
- Mackay N. and Eastburn D. (1990). The Murray. *Murray Darling Basin Commission*. Retrieved from <https://catalogue.nla.gov.au/catalog/249485>
- Marshall G.J. (2003). Trends in the Southern Annular Mode from Observations and Reanalyses, *Journal of Climate*, **16**(24), 4134–4143. Doi: [https://doi.org/10.1175/1520-0442\(2003\)016<4134:TITSAM>2.0.CO;2](https://doi.org/10.1175/1520-0442(2003)016<4134:TITSAM>2.0.CO;2)
- McGowan H.A., Marx S.K., Denholm J., Soderholm J. and Kamber B.S. (2009). Reconstructing annual inflows to the headwater catchments of the Murray River, Australia, using the Pacific Decadal Oscillation. *Geophysical Research Letters*, **36**(6). Doi: <https://doi.org/10.1029/2008GL037049>
- Meneghini B., Simmonds I. and Smith I. N. (2007). Association between Australian rainfall and the Southern Annular Mode. *International Journal of Climatology*, **27**(1), 109–21. Doi: <https://doi.org/10.1002/joc.1370>
- Murphy B.F. and Timbal B. (2008). A review of recent climate variability and climate change in southeastern Australia. *International Journal of Climatology*, **28**(7), 859–879. Doi: <https://doi.org/10.1002/joc.1627>
- Nicholls N. (2010). Local and remote causes of the southern Australian autumn-winter rainfall decline, 1958–2007. *Climate Dynamics*, **34**(6), 835–45. Doi: <https://doi.org/10.1007/s00382-009-0527-6>
- Rehman S.U., Khan K. and Simmonds I. (2019). Links between Tasmanian precipitation variability and the Indian Ocean subtropical high. *Theoretical and Applied Climatology*, **138**(3):1255–67. Doi: <https://doi.org/10.1007/s00704-019-02891-z>
- Rehman S.U. (2014). Influence of Indian Ocean high pressure on streamflow variability over southwestern Australia. *Annals of Geophysics*, **57**(2). Doi: <https://doi.org/10.4401/ag-6398>
- Rehman S. and Iqbal M.J. (2011). The relationship between Indian Ocean High Pressure and runoff variability in the Donnelly River catchment in southwest western Australia: a case study, *The Nucleus*, **48** (3), 213–222. Retrieved from [https://www.researchgate.net/publication/230672947\\_THE\\_RELATIONSHIP\\_BETWEEN\\_INDIAN\\_OCEAN\\_HIGH\\_PRESSURE\\_AND\\_RUNOFF\\_VARIABILITY\\_IN\\_THE\\_DONNELLY\\_RIVER\\_CATCHMENT\\_IN\\_SOUTHWEST\\_WESTERN\\_AUSTRALIA\\_A\\_CASE\\_STUDY](https://www.researchgate.net/publication/230672947_THE_RELATIONSHIP_BETWEEN_INDIAN_OCEAN_HIGH_PRESSURE_AND_RUNOFF_VARIABILITY_IN_THE_DONNELLY_RIVER_CATCHMENT_IN_SOUTHWEST_WESTERN_AUSTRALIA_A_CASE_STUDY)
- Rice J.S. and Emanuel R.E. (2017). How are streamflow responses to the El Niño Southern Oscillation affected by watershed characteristics? *Water Resources Research*, **53**(5), 4393–4406. Doi: <https://doi.org/10.1002/2016WR020097>
- Roemmich D. (2007). Super spin in the southern seas. *Nature*, **449**(7158), 34–35. Doi: <https://doi.org/10.1038/449034a>
- Riemer R., Doherty O.M. and Hameed S. (2006). On the variability of African dust transport across the Atlantic, *Geophysical Research Letter*, **33**. Doi: <https://doi.org/10.1029/2006GL026163>
- Santer B.D. (1988). *Regional validation of general circulation models*, Ph.D. thesis, University of East Anglia, Norwich, England. Retrieved from <https://ui.adsabs.harvard.edu/abs/1987PhDT.425/abstract>
- Sohn E. (2007). The Big Dry. *Science News*. Retrieved from <https://www.sciencenews.org/article/big-dry>

- Stedinger J.R. (1980). Fitting log normal distributions to hydrologic data. *Water Resources Research*, **16**(3), 481–490. Doi: <https://doi.org/10.1029/WR016i003p00481>
- Stokes R.A., Stone K. and Loh I.C. (1980). *Summary of soil salt storage characteristics in the northern Darling Range*. Water Resources Section, Public Works Department West Australia technical report. Retrieved from [https://scholar.google.com/citations?view\\_op=view\\_citation&hl=en&user=YmQ4bs4AAAAJ&citation\\_for\\_view=YmQ4bs4AAAAJ:zYLM7Y9cAGgC](https://scholar.google.com/citations?view_op=view_citation&hl=en&user=YmQ4bs4AAAAJ&citation_for_view=YmQ4bs4AAAAJ:zYLM7Y9cAGgC)
- Verdon-Kidd D.C. and Kiem A.S. (2009). Nature and causes of protracted droughts in southeast Australia: Comparison between the Federation, WWII, and Big Dry droughts. *Geophysical Research Letters*. **36**(22). Doi: <https://doi.org/10.1029/2009GL041067>
- Vu D.H., Muttaqi K.M. and Agalgaonkar A.P. (2015). A variance inflation factor and backward elimination based robust regression model for forecasting monthly electricity demand using climatic variables. *Applied Energy*, **140**, 385–394. Doi: <https://doi.org/10.1016/j.apenergy.2014.12.011>
- Young W.J. (2001). *Rivers as ecological systems: the Murray-Darling Basin Canberra*. Murray Darling Basin Commission. Retrieved from <https://catalogue.nla.gov.au/catalog/2527612>
- Yu Y.S., Zou S. and Whittemore D. (1993). Non-parametric trend analysis of water quality data of rivers in Kansas. *Journal of Hydrology*, **150**(1), 61–80. Doi: [https://doi.org/10.1016/0022-1694\(93\)90156-4](https://doi.org/10.1016/0022-1694(93)90156-4)
- Zhang X., Harvey K.D., Hogg W.D. and Yuzyk T.R. (2001). Trends in Canadian streamflow. *Water Resources Research*, **37**(4), 987–998. Doi: <https://doi.org/10.1029/2000WR900357>